

Fluorescent Organic Nanoparticles of Biginelli-Based Molecules: Recognition of Hg^{2+} and Cl^- in an Aqueous MediumAjnesh Singh,[†] Tilak Raj,[†] Thammarat Aree,[‡] and Narinder Singh^{*,†}[†]Department of Chemistry, Indian Institute of Technology Ropar, Rupnagar, Punjab 140001, India[‡]Department of Chemistry, Faculty of Science, Chulalongkorn University, Bangkok 10330, Thailand

Supporting Information

ABSTRACT: Biginelli-based molecules (1–3) have been synthesized and developed as a new class of fluorescent organic nanoparticle-based chemosensors. Chemosensor 2 has shown excellent selectivity and sensitivity for detection of Hg^{2+} in an aqueous medium. It can detect Hg^{2+} up to 1 nM, and the resultant 2Hg^{2+} complex can detect Cl^- ions (micromolar level) in an aqueous medium.

The development and synthesis of fluorescent organic nanoparticles (FONPs) have received increased attention from chemists in recent years.^{1–4} Advances in the field of FONPs have equipped chemists with new tools because of their chemical, biochemical, and technological applications.^{5–8} Compared to metallic nanoparticles, FONPs are expected to offer higher potentials because organic material allows much more variability and flexibility through well-known synthetic skills.^{9,10} Moreover, FONPs dispersed in water authenticate the use of probes in biological samples. Nakanishi et al. have reported systematic work on FONPs with the use of perylene and phthalocyanin nanoparticles that revealed the size-dependent fluorescent properties of organic materials.¹¹ Although many research groups have reported marvelous properties of FONPs, nevertheless, the field is at a juvenile stage only and much progress is still within the scope. Inspired by the great potential of FONPs for chemosensor development, we have developed a new class of organic compounds that aggregate into FONPs and act as excellent chemosensors in an aqueous medium.⁵ Moreover, in the recent years, detection of anions, cations, or biomolecules has gained main importance because of the significance of detecting target species in biological and environmental samples.¹²

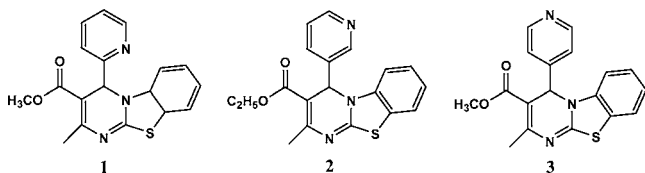
We have synthesized Biginelli-based compounds (1–3; Scheme 1) by employing one-pot multicomponent organic synthesis. Compounds 1–3 were synthesized by refluxing 2-aminobenzothiazole, arylaldehyde, and β -ketoesters in methanol containing a catalytic amount of $\text{Zn}(\text{ClO}_4)_2$. The structures of 1–3 were established by elemental analysis and ^1H and ^{13}C NMR

and Fourier transform infrared spectroscopies (Figures S1–S6 in the Supporting Information, SI). The structures of 1–3 were also optimized by density functional theory calculations (Figure S7 in the SI). FONPs of 1–3 were prepared by a reprecipitation method.¹³

The photophysical properties of FONPs in an aqueous medium showed clear deviation from that of receptors (1–3) in pure acetonitrile (Figure S8 in the SI). Interestingly, the fluorescence intensity of FONPs of 1 decreased, while it increased up to 2-fold in the case of FONPs of 2 and 3. This change in the emission behavior of organic molecules upon formation of nanoaggregates/nanoparticles may be ascribed to the restriction of intramolecular rotation, nonradiative decay, excimer formation, etc.^{14,15} Also, the formation of nanoparticles was confirmed by dynamic light scattering (DLS) studies. DLS analysis showed organic nanoparticles of size 74, 28, and 32 nm in 1–3, respectively (Figures S9–S11 in the SI).

In an effort to develop FONPs of 1–3 as chemosensors in an aqueous medium, their cation recognition behavior was evaluated from changes in the UV–vis and fluorescence spectra upon the addition of a particular metal salt (100 μM) to a solution of FONPs (20 μM) of the respective receptor in a Tris buffer (pH 7.4, 1 mM). FONPs of 1 have not shown any selectivity for tested metal ions (Figure S12 in the SI). In the case of FONPs of 2, interesting results were obtained; i.e., the addition of Hg^{2+} ions to FONPs of 2 resulted in a significant change in the UV–vis spectrum with the appearance of a new band at 345 nm and diminishing of the band at 386 nm. The addition of other metal ions caused only minor changes in the UV–vis spectrum under the same conditions (Figure S13 in the SI). These changes in the photophysical properties upon the addition of Hg^{2+} offer ratiometric recognition of environmentally harmful Hg^{2+} ions in an aqueous medium.¹⁶ A similar behavior was observed with FONPs of 3 (Figure S14 in the SI) for Hg^{2+} , but interference was observed from Cu^{2+} ; therefore, in the present work, only FONPs of 2 are studied in detail and termed chemosensor 2 in a further discussion. To gain more insight into the binding behavior, titration of chemosensor 2 with Hg^{2+} was performed (Figure 1A). The addition of successive increased amounts (0–100 μM) of Hg^{2+} to chemosensor 2 resulted in a continuous increase at 345 nm and a decrease in the band at 386 nm with an isosbestic point at 369 nm. These changes can be explained on the basis that when Hg^{2+} ions coordinate with S and N atoms of the $\text{C}=\text{N}$ group, it led to a decrease in absorbance at 386 nm and the formation of a

Scheme 1. Structures of Compounds 1–3



Received: November 5, 2013

Published: December 3, 2013

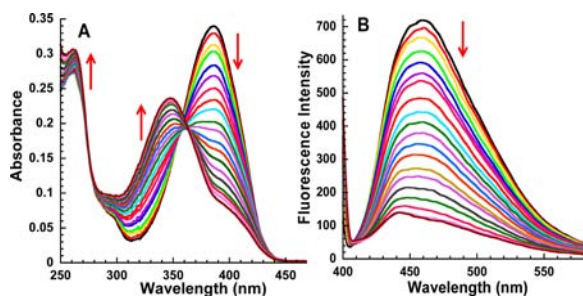


Figure 1. (A) Changes in the UV–vis absorption spectra of chemosensor **2** ($40 \mu\text{M}$) in a Tris buffer upon the addition of Hg^{2+} from 0 to $100 \mu\text{M}$. (B) Changes in the fluorescent spectra ($\lambda_{\text{ex}} = 386 \text{ nm}$) of chemosensor **2** ($40 \mu\text{M}$) in a Tris buffer upon the addition of Hg^{2+} from 0 to $100 \mu\text{M}$.

new band at 345 nm because of a ligand-to-metal charge-transfer transition. These data offer a ratiometric estimation of Hg^{2+} with a linear response in the range of $20\text{--}30 \mu\text{M}$ of added Hg^{2+} and $A_{345 \text{ nm}}/A_{386 \text{ nm}}$ (Figure S15). To test the practical applicability of chemosensor **2** as a Hg^{2+} -selective chromogenic sensor, competitive experiments were carried out (Figure S16) and clearly depict that no interference was offered by other metal ions, meaning that chemosensor **2** has a high selectivity for Hg^{2+} ions in an aqueous medium.

Also, the emission studies of chemosensor **2** showed excellent selectivity toward Hg^{2+} ions (Figure S17), and the addition of Hg^{2+} resulted in quenching of the emission band at $\lambda_{\text{max}} = 456 \text{ nm}$ with a shift in λ_{max} to 440 nm . This shift/quenching of the emission wavelength might be ascribed to a conformational change in chemosensor **2** and the intramolecular charge-transfer process. Coordination of Hg^{2+} with chemosensor **2** probably results in distortion of the rigid confirmation attained during the formation of FONPs, which led to quenching of the intensity. As in **2**, the fluorophore and binding sites are directly bound to each other, and interaction of Hg^{2+} ions with lone pair of N/S atoms disturbs the electron cloud of fluorophore, which led to quenching of fluorescence with a blue shift. To understand the binding behavior of Hg^{2+} , titration of chemosensor **2** in a Tris buffer with Hg^{2+} was performed (Figure 1B and Figure S18). A successive increase in the amount of Hg^{2+} ($0\text{--}100 \mu\text{M}$) resulted in a continuous decrease in the fluorescence intensity at 456 nm with a shift in the band to 440 nm . The minimum detection limit was found to be 1 nM (3σ slope method).¹⁷ A series of competitive experiments (Figure S19) showed that chemosensor **2** can selectively recognize Hg^{2+} in the presence of other competing ions. A comparison of the present and reported chemosensors is given in Table S1 in the SI. The time-dependent changes in the UV–vis spectra upon the addition of Hg^{2+} ions ($100 \mu\text{M}$) to a solution of chemosensor **2** ($40 \mu\text{M}$) showed that the response time of the probe is low and no changes were noticed in the spectra after the first 3 min (Figure S20). Perturbation of the high ionic strength was ruled out by a comparison of the UV–vis and fluorescence spectra of chemosensor **2** (Figure S21).

It is well-known that the pH has a great influence on the properties of any sensing probe, and for better utility of the probe, it should show the same behavior in a wide pH range. The effect of the pH on the absorption and emission profiles of chemosensor **2** showed interesting results (Figures S22, S23). Chemosensor **2** was stable in neutral, basic ($7\text{--}12$), and less acidic ($7\text{--}6$) pH ranges; however, at lower pH, the UV–vis and emission profiles observed were quite identical with that observed during titration of chemosensor **2** with Hg^{2+} ions. Encouraged by the pH titration results, we tried to grow single crystals of **2** in the presence of some

protic acids like HCl, HBr, and HClO_4 to understand the binding mechanism. Single crystals were obtained from an acetone/ H_2O mixture of **2** containing a few drops of perchloric acid. Our repeated attempts to grow single crystals of the $2\cdot\text{Hg}^{2+}$ complex were not successful.

Single-crystal X-ray diffraction studies revealed the formation of complex $2\cdot\text{H}^+\cdot\text{ClO}_4^-$, which crystallizes in an orthorhombic crystal system with a *Pbca* space group. The asymmetric unit contains one protonated moiety of **2** and one perchlorate anion. Here the N2 atom of **2** was protonated, and the charge was balanced by the perchlorate anion (Figure 2). Packing analysis

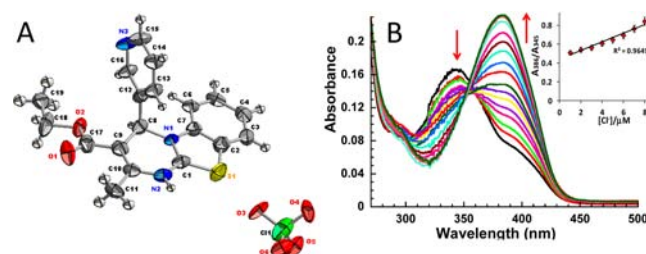


Figure 2. (A) ORTEP diagram of $2\cdot\text{H}^+\cdot\text{ClO}_4^-$. (B) Changes in UV–vis absorption spectrum of $2\cdot\text{H}^+$ on addition of Cl^- ($0\text{--}15 \mu\text{M}$).

(Figure S24) clearly shows that the N–H group of the benzothiazole moiety forms a strong N–H \cdots N hydrogen bond [$\text{N2}\text{--}\text{H2A}\cdots\text{N3} = 1.957(3)^\circ$] with the pyridine N3 atom. The O3 atom of the perchlorate ion has short contact with the S1 atom of the benzothiazole moiety.

Further, the $2\cdot\text{Hg}^{2+}$ complex was investigated as a secondary sensor for anion recognition (the solution obtained after titration of chemosensor **2** with Hg^{2+} was used as is). This method offers a sporadic opportunity to recognize any anion in an aqueous medium.¹⁸ Interestingly, the addition of Cl^- ($100 \mu\text{M}$) led to significant changes in the UV–vis spectrum (Figure S25). The band at 345 nm disappeared, while a new band was appeared at 386 nm . In other words, the addition of Cl^- led to complete restoration of the spectrum to the stage before the interaction of chemosensor **2** with Hg^{2+} ions. However, no such significant changes were observed with other tested anions. The Cl^- -dependent UV–vis response of $2\cdot\text{Hg}^{2+}$ was recorded upon the addition of successive amounts ($0\text{--}15 \mu\text{M}$) of a Hg^{2+} solution (Figure 2B). As per expectations, the enhancement in absorbance at 386 nm is directly proportional to $[\text{Cl}^-]$ within the concentration range of $1\text{--}8 \mu\text{M}$ (Figure 2B, inset). Using this data, Cl^- can be detected up to $2 \mu\text{M}$. Competitive experiments confirmed the high selectivity of the $2\cdot\text{Hg}^{2+}$ complex for the Cl^- ion (Figure S26).

Regarding the mechanism of recognition of Hg^{2+} , it is believed that Hg^{2+} metal ion interacts with the lone pair of the N atom similarly to that of H^+ , resulting in similar absorption/emission profiles. Also, the decrease in the fluorescence intensity is the result of a disturbance in the conjugation of a π -electron cloud due to involvement of the N atom in bonding with a $\text{Hg}^{2+}/\text{H}^+$ ion. This phenomenon is further supported by NMR titration. Although a significant chemical shift has been observed in all of the aromatic protons, most of the effected protons are in close vicinity of the bonding N atom. ^1H NMR titrations were performed by varying the mole ratio between Hg^{2+} and **2** from 0 to 2 (Figure S27 in the SI). A shift of $\Delta\delta = 0.07, 0.18, \text{ and } 0.05$ was observed in signals at $\delta 6.75$ (s, 1H, $-\text{CH}$), 8.88 (s, 1H, ArH), 8.07 (d, 1H, ArH). All of these protons are at close vicinity of the ring containing the N atom coordinating to Hg^{2+} . Moreover, the

splitting of a singlet at δ 6.75 and a multiplet at δ 7.46–7.35 indicates the unsymmetrical mode of binding of ligands to the metal center.

The formation of the $2\cdot\text{Hg}^{2+}$ complex and its interaction with the Cl^- anion were also studied by cyclic voltammetry and differential pulse voltammetry; it was found that the addition of Cl^- to the $2\cdot\text{Hg}^{2+}$ complex gave a profile different from that of chemosensor **2** and its Hg^{2+} complex (Figures S28 and S29 in the SI), which illustrates that Cl^- replaces some ion/molecule from the $2\cdot\text{Hg}^{2+}$ coordination sphere rather than extracting the Hg^{2+} ion from the $2\cdot\text{Hg}^{2+}$ complex; therefore, different profiles were observed. The electrochemical studies and results obtained from interaction of the $2\cdot\text{Hg}^{2+}$ complex with thiol/ethylenediaminetetraacetic acid (Figure S28 in the S30) indicated that the addition of Hg^{2+} ions (as a nitrate salt) to chemosensor **2** led to the formation of complex $2\cdot\text{Hg}^{2+}\cdot(\text{NO}_3^-)_2$. The NO_3^- ions were removed from the coordination sphere of the mercury complex as soon as Cl^- ions were added to the solution of the mercury complex. It is believed that orientation of the ligands around Hg^{2+} is so that only a particular size of Cl^- ions is conducive to interacting selectively with the metal ion. Thus, our mercury complex acts as a secondary sensor for Cl^- through counterion displacement assay.

In conclusion, three new Biginelli-based receptors **1–3** were synthesized and characterized. FONPs of **1–3** have been prepared and developed as chemosensors. FONPs of **2** can selectively recognize Hg^{2+} in an aqueous medium, and the resultant $2\cdot\text{Hg}^{2+}$ complex acts as a secondary sensor for Cl^- ions through counterion displacement assay. The mechanism of Hg^{2+} binding was established from the crystal structure of $2\cdot\text{H}^+\cdot\text{ClO}_4^-$, ^1H NMR titration, and electrochemical studies.

■ ASSOCIATED CONTENT

📄 Supporting Information

Experimental details, NMR spectra, recognition studies, and X-ray crystallographic data in CIF format (CCDC 954989). This material is available free of charge via the Internet at <http://pubs.acs.org>.

■ AUTHOR INFORMATION

Corresponding Author

*E-mail: nsingh@iitrpr.ac.in.

Notes

The authors declare no competing financial interest.

■ ACKNOWLEDGMENTS

Work was supported by CSIR, New Delhi, India [Grant 01(2417)/10/EMR-II], with partial financial support from the Chulalongkorn University Centenary Academic Development Project (CUS6-FW10) and the National Research University Project (FW657B).

■ REFERENCES

- (1) Xi, L.; Fu, H.; Yang, W.; Yao, J. *Chem. Commun.* **2005**, 492–494.
- (2) Sun, Y.-Y.; Liao, J.-H.; Fang, J.-M.; Chou, P.-T.; Shen, C.-H.; Hsu, C.-W.; Chen, L.-C. *Org. Lett.* **2006**, *8*, 3713–3716.
- (3) An, B.-K.; Kwon, S.-K.; Park, S. *Angew. Chem., Int. Ed.* **2007**, *46*, 1978–1982.
- (4) Jana, A.; Sanjana, K.; Devi, P.; Maiti, T. K.; Pradeep, N. D. S. *J. Am. Chem. Soc.* **2012**, *134*, 7656–7659.
- (5) (a) Xu, X.; Li, J.; Li, Q.; Huang, J.; Dong, Y.; Hong, Y.; Yan, J.; Qin, J.; Li, Z.; Tang, B. Z. *Chem.—Eur. J.* **2012**, *18*, 7278–7286. (b) Petkau, K.; Kaeser, A.; Fischer, I.; Brunsveld, L.; Schenning, A. P. H. J. *J. Am. Chem.*

Soc. **2011**, *133*, 17063–17071. (c) Li, H.; Xu, J.; Yan, H. *Sens. Actuators, B* **2009**, *139*, 483–487.

(6) Mei, J.; Tong, J.; Wang, J.; Qin, A.; Sun, J. Z.; Tang, B. Z. *J. Mater. Chem.* **2012**, *22*, 17063–17070.

(7) Kim, H.-J.; Lee, J.; Kim, T.-H.; Lee, T. S.; Kim, J. *Adv. Mater.* **2008**, *20*, 1117–1121.

(8) Lin, H. H.; Su, S. Y.; Chang, C. C. *Org. Biomol. Chem.* **2009**, *7*, 2036–2039.

(9) Kang, L.; Chen, Y.; Xiao, D.; Peng, A.; Shen, F.; Kuang, X.; Fu, H.; Yao, J. *Chem. Commun.* **2007**, 2695–2697.

(10) McDonald, T. O.; Martin, P.; Patterson, J. P.; Smith, D.; Giardiello, M.; Marcello, M.; See, V.; O'Reilly, R. K.; Owen, A. *Adv. Funct. Mater.* **2012**, *22*, 2469–2478.

(11) (a) Kasai, H.; Kamatani, H.; Yoshikawa, Y.; Okada, S.; Oikawa, H.; Watanabe, A.; Ito, O.; Nakanishi, H. *Chem. Lett.* **1997**, 1181–1182.

(b) Komai, Y.; Kasai, H.; Hirakoso, H.; Hakuta, Y.; Okada, S.; Oikawa, H.; Adschiri, T.; Inomata, H.; Arai, K.; Nakanishi, H. *Mol. Cryst. Liq. Cryst.* **1998**, *322*, 167–172.

(12) (a) Mikata, Y.; Ugai, A.; Ohnishi, R.; Konno, H. *Inorg. Chem.* **2013**, *52*, 10223–10225. (b) Santos-Figueroa, L. E.; Moragues, M. E.; Raposo, M. M. M.; Batista, R. M. F.; Costa, S. P. G.; Ferreira, R. C. M.; Sancenón, F.; Martínez-Máñez, R.; Ros-Lis, J. V.; Soto, J. *Org. Biomol. Chem.* **2012**, *10*, 7418–7428. (c) Lee, D. Y.; Singh, N.; Kim, M. J.; Jang, D. O. *Org. Lett.* **2011**, *13*, 3024–3027.

(13) Al-Kaysi, R. O.; Müller, A. M.; Ahn, T. S.; Lee, S.; Bardeen, C. J. *Langmuir* **2005**, *21*, 7990–7994.

(14) (a) Hong, Y.; Lam, J. W. Y.; Tang, B. Z. *Chem. Commun.* **2009**, 4332–4353. (b) MacDiarmid, A. G.; Epstein, A. J. *Phys. Rev. B* **1996**, *54*, 9180–9189.

(15) Yagai, S.; Goto, Y.; Lin, X.; Karatsu, T.; Kitamura, A.; Kuzuhara, D.; Yamada, H.; Kikkawa, Y.; Saeki, A.; Seki, S. *Angew. Chem., Int. Ed.* **2012**, *51*, 6643–6647.

(16) (a) Liu, D.; Qu, W.; Chen, W.; Zhang, W.; Wang, Z.; Jiang, X. *Anal. Chem.* **2010**, *82*, 9606–9610. (b) Lee, J.-S.; Han, M. S.; Mirkin, C. A. *Angew. Chem., Int. Ed.* **2007**, *46*, 4093–4096. (c) Zhan, X.-Q.; Qian, Z.-H.; Zheng, H.; Su, B.-Y.; Lan, Z.; Xu, J.-G. *Chem. Commun.* **2008**, 1859–1861.

(17) Zhu, M.; Yuan, M. J.; Liu, X. F.; Xu, J. L.; Lv, J.; Huang, C. S.; Liu, H. B.; Li, Y. L.; Wang, S.; Zhu, D. B. *Org. Lett.* **2008**, *10*, 1481–1484.

(18) (a) Hancock, L. M.; Beer, P. D. *Chem.—Eur. J.* **2008**, *15*, 42–44. (b) Comes, M.; Aznar, E.; Moragues, M.; Marcos, M. D.; Martínez-Máñez, R.; Sancenón, F.; Soto, J.; Villaescusa, L. A.; Gil, L.; Amorós, P. *Chem.—Eur. J.* **2009**, *15*, 9024–9033.